Quantum interference of V-type three-level atom in structures made of left-handed materials and mirrors

Jing-ping Xu and Ya-ping Yang
Department of Physics, Tongji University, Shanghai 200092, People's Republic of China
(Received 26 June 2009; published 25 January 2010)

We address quantum interference of the Zeeman atom embedded in two kinds of structures containing left-handed materials (LHM), which are a single LHM layer mounted on a single mirror (SLSM) and Fabry-Pérot cavity filled with a LHM layer by half (FPCLH). Especially, the influence of the dissipation of LHM on quantum interference has been studied in detail. Though dissipation weakens quantum interference in general, it holds nearly complete quantum interference when the thickness of the cavity is small for FPCLH. Moreover, with equivalence of left- and right- rotation polarized dipoles to two spatial orthogonal dipoles, we found the optimum orientation of two orthogonal dipoles which can realize the maximum quantum interference in a certain anisotropic environment. Our research may have potential applications in the designing of microsize devices.

DOI: 10.1103/PhysRevA.81.013816 PACS number(s): 42.50.Gy, 32.60.+i, 42.50.Ct

I. INTRODUCTION

The quantum interference among different decay channels of the atom has attracted great attention for a long time [1–6], since it results in many fascinating phenomena in the field of laser and quantum information, such as coherence trapping of population [1], lasing without inversion [2], electromagnetically induced transparency [3], atomic excited level population trapping [4], ultranarrow spectral line [5], and gain without inversion [6]. However, strong quantum interference requires the presence of near-degenerate atomic transitions with near-(anti)parallel dipole moments sharing a common atomic state. It is well known that the near-degenerate atomic transitions can be realized through the Zeeman splitting, but the corresponding dipole moments are orthogonal to each other, in which one is left-rotation polarized and the other is right-rotation polarized. Therefore, there is rarely experimental proof of strong quantum interference in atomic systems due to the lack of an appropriate candidate system.

To avoid the difficulty in quantum interference of the atomic system, Agarwal [7] first suggested that quantum interference between two orthogonal dipole moments can be revived in an anisotropic vacuum. Later, the anisotropy of a multilayer dielectric medium [8] and one-dimensional photonic crystals [9] has been checked, and the quantum interferences of a Zeeman V-type atom in these environments have been studied theoretically. However, the required distance between atom and interface of those structures for strong quantum interference cannot be larger than half of the wavelength, equivalently the width of the space with high anisotropy in Refs. [7–9] is less than half of the wavelength at the atomic transition frequency, which is a strong constraint for experiment.

Recently, we published a paper emphasizing that the Zeeman atom could have strong quantum interference in a much wider space with the help of left-handed materials (LHM) [10] due to the enhanced indirect quantum interference. LHM introduced by Veselago in 1968 [11] refer to the materials possessing negative permittivity, negative permeability, and negative refractive index simultaneously at interesting frequencies. With its significant advantage of phase compensation, LHM has promising applications in perfect lens [12], the sub-wavelength cavity resonator [13], and complete inhibition of spontaneous decay [14]. Until now, LHM had been fabricated in the microwave region, infrared, and visible light frequencies [15,16].

Here, based on the content of Ref. [10], we explore the influence of the dissipation of LHM on the quantum interference in detail, and analyze the quantum interference between two spatial orthogonal dipole moments in a certain environment. This paper is arranged as follows. In Sec. II, we give the principle of reviving the quantum interference of the Zeeman atom in an anisotropic vacuum. In Sec. III, we discuss the quantum interference of the Zeeman atom embedded in two kinds of structure, i.e., SLSM and FPCLH, especially focusing on the influence of dissipation on quantum interference. In Sec. IV, the necessary condition required for strong quantum interference of two spatial orthogonal decay channels is analyzed. Section V draws our conclusion.

II. QUANTUM INTERFERENCE OF A ZEEMAN THREE-LEVEL ATOM

We consider a V-type three-level atom located in a one-dimensional structure, which is shown in Fig. 1. The layer containing the atom is a vacuum, which is marked by "Layer 0" with thickness d_0. The center of Layer 0 is taken as the origin of the coordinate. The atom with position $(0, 0, z_0)$ has two closely lying upper states $|1\rangle$ and $|2\rangle$, and one ground state $|3\rangle$. For the Zeeman atom, the atomic dipole moment operator is represented by $\mathbf{d} = d(A_{13}\boldsymbol{\varepsilon}_- + A_{23}\boldsymbol{\varepsilon}_+) + \text{H.c.}$, in which $\boldsymbol{\varepsilon}_+ = (\boldsymbol{e}_z + i\boldsymbol{e}_x)/\sqrt{2}$ and $\boldsymbol{\varepsilon}_- = (\boldsymbol{e}_z - i\boldsymbol{e}_x)/\sqrt{2}$ refer to right-rotating and left-rotating unit vectors, respectively. $A_{ij} = |i\rangle\langle j|(i, j = 1, 2, 3)$ is the atomic operator, and the amplitude of the dipole moment d is chosen to be real.

According to Ref. [8], the simultaneous equations of the expectation values of atomic operators for the V-type three-level atom are

$$\frac{d}{dt}\langle A_{11}\rangle = -2\gamma_1\langle A_{11}\rangle - \kappa_2\langle A_{12}\rangle - \kappa_2\langle A_{21}\rangle, \quad (1)$$

$$\frac{d}{dt}\langle A_{22}\rangle = -2\gamma_2\langle A_{22}\rangle - \kappa_1\langle A_{21}\rangle - \kappa_1\langle A_{12}\rangle, \quad (2)$$

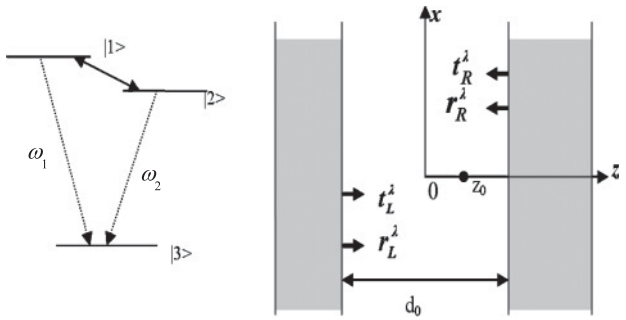

FIG. 1. The V-type three-level atom (left figure) is placed in the one-dimensional structure (right figure).

$$\frac{d}{dt}\langle A_{12}\rangle = -[\gamma_1+\gamma_2+i(\omega_2-\omega_1)]\langle A_{12}\rangle - \kappa_1\langle A_{11}\rangle - \kappa_2\langle A_{22}\rangle, \tag{3}$$

where

$$\gamma_1 = d^2\omega_1^2\boldsymbol{\varepsilon}_-\cdot \mathrm{Im}\overleftrightarrow{\boldsymbol{G}}(\boldsymbol{r}_0,\boldsymbol{r}_0,\omega_1)\cdot\boldsymbol{\varepsilon}_+ = d^2\omega_1^2\,\mathrm{Im}[G_{zz}(\boldsymbol{r}_0,\boldsymbol{r}_0,\omega_1)+G_{xx}(\boldsymbol{r}_0,\boldsymbol{r}_0,\omega_1)]/2, \tag{4}$$

$$\gamma_2 = d^2\omega_2^2\boldsymbol{\varepsilon}_-\cdot \mathrm{Im}\overleftrightarrow{\boldsymbol{G}}(\boldsymbol{r}_0,\boldsymbol{r}_0,\omega_2)\cdot\boldsymbol{\varepsilon}_+ = d^2\omega_2^2\,\mathrm{Im}[G_{zz}(\boldsymbol{r}_0,\boldsymbol{r}_0,\omega_2)+G_{xx}(\boldsymbol{r}_0,\boldsymbol{r}_0,\omega_2)]/2, \tag{5}$$

$$\kappa_1 = d^2\omega_1\omega_2\boldsymbol{\varepsilon}_+\cdot \mathrm{Im}\overleftrightarrow{\boldsymbol{G}}(\boldsymbol{r}_0,\boldsymbol{r}_0,\omega_1)\cdot\boldsymbol{\varepsilon}_+ = d^2\omega_1\omega_2\,\mathrm{Im}[G_{zz}(\boldsymbol{r}_0,\boldsymbol{r}_0,\omega_1)-G_{xx}(\boldsymbol{r}_0,\boldsymbol{r}_0,\omega_1)]/2, \tag{6}$$

$$\kappa_2 = d^2\omega_1\omega_2\boldsymbol{\varepsilon}_-\cdot \mathrm{Im}\overleftrightarrow{\boldsymbol{G}}(\boldsymbol{r}_0,\boldsymbol{r}_0,\omega_2)\cdot\boldsymbol{\varepsilon}_- = d^2\omega_1\omega_2\,\mathrm{Im}[G_{zz}(\boldsymbol{r}_0,\boldsymbol{r}_0,\omega_2)-G_{xx}(\boldsymbol{r}_0,\boldsymbol{r}_0,\omega_2)]/2. \tag{7}$$

In which γ_1 and γ_2 are the spontaneous decay rates for transitions $|1\rangle \to |3\rangle$ and $|2\rangle \to |3\rangle$, respectively. κ_1 and κ_2 are the quantum interference between two decay channels. In the presence of quantum interferences κ_1 and κ_2, $\langle A_{11}\rangle$ and $\langle A_{22}\rangle$ do not decay with the decay rate γ_1 and γ_2 according to Eqs. (1) and (2).

In a free vacuum, the Green tensor $\overleftrightarrow{\boldsymbol{G}}(\boldsymbol{r}_0,\boldsymbol{r}_0,\omega)$ is isotropic, i.e., $G_{xx}=G_{yy}=G_{zz}$, therefore quantum interference does not happen (κ_1 and κ_2 are zero). However, if the vacuum is anisotropic, i.e., $G_{zz}\neq G_{xx}$, then quantum interference $\kappa_1(\kappa_2)$ appears. We adopt the relative strength of quantum interference $p=\kappa_n/\sqrt{\gamma_1\gamma_2}$ [8] to measure quantum interference. Because the two Zeeman upper levels are nearly degenerate, the approximation $\omega_1\approx\omega_2=\omega_0$ is reasonable. With the definition of $\Gamma_\perp = d^2\omega_0^2\mathrm{Im}G_{zz}(r_0,r_0,\omega_0)$ and $\Gamma_{||} = d^2\omega_0^2\,\mathrm{Im}G_{xx}(r_0,r_0,\omega_0)$, p becomes

$$p=\frac{\Gamma_\perp-\Gamma_{||}}{\Gamma_\perp+\Gamma_{||}}. \tag{8}$$

Here $\Gamma_\perp$ is the spontaneous decay rate of the dipole momentum $\boldsymbol{d}$ perpendicular to the interface, i.e., along the z-axis, and $\Gamma_{||}$ is the spontaneous decay rate of the dipole momentum d parallel to the interface, i.e., along the x-axis. It is clear that p increases with the difference between $\Gamma_\perp$ and $\Gamma_{||}$. If $\Gamma_{||}=0$, we get $p=1$ with $\gamma_1=\gamma_2=\kappa_1=\kappa_2=\Gamma_\perp/2$, which means complete quantum interference happens. With the help of the Green tensor in a multilayer [17], the decay rate $\Gamma_\perp$ and $\Gamma_{||}$ can be expressed as

$$\Gamma_{||} = \frac{3}{4}\Gamma_0\mathrm{Re}\left(\int_0^K+\int_K^\infty\right)\frac{d\beta}{K}\frac{\beta}{K_z}\left\{\left[1+\frac{2r_L^{TE}r_R^{TE}e^{i2K_zd_0}+r_L^{TE}e^{iK_z(d_0+2z_a)}+r_R^{TE}e^{iK_z(d_0-2z_a)}}{D_{TE}}\right]+\frac{K_z^2}{K^2}\left[1+\frac{2r_L^{TM}r_R^{TM}e^{i2K_zd_0}-r_L^{TM}e^{iK_z(d_0+2z_a)}-r_R^{TM}e^{iK_z(d_0-2z_a)}}{D_{TM}}\right]\right\} = \Gamma_{||\mathrm{rad}}+\Gamma_{||\mathrm{nonrad}}, \tag{9}$$

$$\Gamma_\perp = \frac{3}{2}\Gamma_0\mathrm{Re}\left(\int_0^K+\int_K^\infty\right)\frac{d\beta}{K_z}\frac{\beta^3}{K^3}\left[1+\frac{2r_L^{TM}r_R^{TM}e^{i2K_zd_0}+r_L^{TM}e^{iK_z(d_0+2z_a)}+r_R^{TM}e^{iK_z(d_0-2z_a)}}{D_{TM}}\right] = \Gamma_{\perp\mathrm{rad}}+\Gamma_{\perp\mathrm{nonrad}}. \tag{10}$$

Here $\Gamma_0=d^2\omega_0^3/(3\pi\varepsilon_0\hbar c^3)$ is the decay rate of dipole moment $\boldsymbol{d}$ at ω_0 in free space. Two components of the wave vector, the z-component K_z and the projection on the x-y plane β, satisfy the relationship of $K_z^2+\beta^2=K^2$, in which $K=\omega_0/c$ is the wave number. $r_R^q(r_L^q)$ is the reflective coefficient at the right (left) interface of Layer 0 for polarization $q=TE$ or TM. D_q originates from the multireflection in Layer 0, which is

$$D_q = 1-r_L^qr_R^qe^{2iK_zd_0}. \tag{11}$$

In Eqs. (9) and (10), the decay rate is divided into two parts: the radiative decay rate and nonradiative decay rate. Radiative decay refers to the decay through an emitting photon, which is embodied by integration over β from 0 to K. Nonradiative decay originates from a Coulomb interaction between the atom and its surrounding, and happens only when the surrounding contains dissipation. In mathematics, nonradiative decay rate is embodied by integration over β from K to infinite in Eqs. (9) and (10) while K_z is a pure imaginary number.

III. QUANTUM INTERFERENCE OF ZEEMAN ATOM EMBEDDED IN THE STRUCTURE CONTAINING LHM

Agarwal [8] first pointed out that anisotropy may lead to quantum interference between two orthogonal dipole moments. He adopted the ideal Fabry-Pérot cavity (FPC) (cavity with two perfect mirrors) to construct a high anisotropic space,

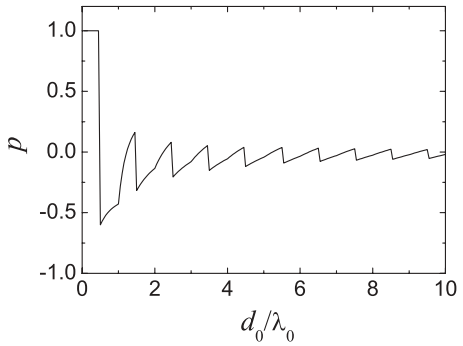

FIG. 2. The relative strength of the quantum interference p as a function of the width of the cavity for ideal cavity, $z_0 = 0$.

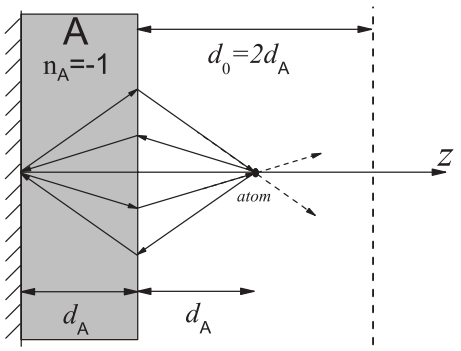

FIG. 3. The atom is in front of a single LHM layer mounted on a single mirror.

and gave spontaneous decay rates in such a cavity as [8]

$$\Gamma_\perp/\Gamma_0 = \frac{3\pi}{2Kd_0} + \frac{3\pi}{Kd_0}\sum_{n=1}^{N}\left(1-\frac{\pi^2n^2}{K^2d_0^2}\right) \times \cos^2\left(\frac{z_0+d_0/2}{d_0}\pi n\right), \tag{12}$$

$$\Gamma_{||}/\Gamma_0 = \frac{3\pi}{2Kd_0}\sum_{n=1}^{N}\left(1+\frac{\pi^2n^2}{K^2d_0^2}\right)\sin^2\left(\frac{z_0+d_0/2}{d_0}\pi n\right). \tag{13}$$

Here N is the largest integer which is smaller than Kd_0/π. If $d_0 < \lambda_0/2$, and then $\Gamma_{||} = 0$ and $\Gamma_\perp/\Gamma_0 = 3\pi/(2Kd_0)$, which results in $p = 1$ according to Eq. (8). Otherwise when $d_0 \geqslant \lambda_0/2$, $\Gamma_{||}$ is no longer zero, thus the relative strength p is smaller than 1. p versus d_0 for $z_0 = 0$ in an ideal FPC has been plotted in Fig. 2.

From Fig. 2, it is clear that p is near 1 only when the width d_0 is less than half of the wavelength. With increasing d_0, the amplitude of p decreases. When d_0 is larger than $2\lambda_0$, $|p|$ is less than 0.2 and quantum interference nearly does not work.

A. Single LHM layer mounted on single mirror (SLSM)

In order to hold the strong quantum interference for larger d_0, we try to construct an environment which can inhibit the decay of the x-component dipole even if the distance between the atom and interface is large. Kästel and Fleischhauer [14] pointed out that the structure made of a mirror and a LHM layer has the power to suppress spontaneous emission over a macroscopic distance, which is shown in Fig. 3. The distance between the atom and the right interface of the LHM layer is given exactly as the thickness of the LHM layer d_A. In order to make use of Eqs. (9) and (10) to perform the calculation, we assume a virtual wall on the right side of the atom, see the dotted line in Fig. 3, then $d_0 = 2d_A$.

When Layer A is made of the ideal LHM ($\varepsilon_A = \mu_A = n_A = -1$), the coefficients in Eqs. (9) and (10) take the values as $z_0 = 0$, $r_R^{TM/TE} = 0$, $r_L^{TE} = -\exp(-i2K_zd_A)$, and $r_L^{TM} = \exp(-i2K_zd_A)$. Consequently, we get $p = 1$ with $\Gamma_\perp = 2\Gamma_0$ and $\Gamma_{||} = 0$ for arbitrary d_A (d_0). That means, even if the Zeeman atom is far away from the LHM layer, there is still strong quantum interference.

The result of $p = 1$ originates from the phase compensation of LHM. As the refractive index of LHM layer is -1, the total optical distance between the atom and mirror is $n_Ad_A + d_A = 0$. Therefore the atom is equivalent to be placed just at the mirror. It is well known that, when the atom is placed at the mirror, the density of state for an atom with dipole moment parallel to mirror is zero, while the density of state for an atom with dipole moment normal to mirror is twice of that in free space. As a result, for the Zeeman atom placed in the environment of Fig. 3, we get $\Gamma_{||} = 0$ and $\Gamma_\perp = 2\Gamma_0$. Consequently, the anisotropy of $\Gamma_{||}$ and $\Gamma_\perp$ leads to complete quantum interference as expected.

However, according to the Krames-Kronig relation and the fact that the LHM frequency band is always near the resonance frequency of material [15], the dissipation of LHM cannot be omitted, and then the influence of the LHM's dissipation on quantum interference must be taken into account.

Here we set $\varepsilon_A(\omega_0) = \mu_A(\omega_0) = n_A(\omega_0) = -0.999 + i0.003$, $r_R^{TE/TM} = 0$, and the reflective coefficients of the mirror are $r_{\rm mir}^{TE} = -0.99$ and $r_{\rm mir}^{TM} = 0.99$. The purpose of adopting the above parameters is to realize such refractive index, whose real part is near -1 and its imaginary part is very small at the atomic transition frequency ω_0. Here $\boldsymbol{\varepsilon}_A(\omega_0)$ is chosen to have the same value as $\mu_A(\omega_0)$ in order to weaken the reflection between vacuum and LHM. With Eqs. (8)–(10), we plot p, $\Gamma_{||}$, and $\Gamma_\perp$ as a function of d_0 in Fig. 4.

From Fig. 4(a), with increasing d_0, p decreases from 1 to 0.34 at first, and then increases to maximum 0.8 at $d_0 \approx 1.2\lambda_0$, finally decreasing monotonously to 0.4 at $d_0 = 10\lambda_0$. Such behavior is determined by the properties of $\Gamma_{||}$ and $\Gamma_\perp$.

When d_0 (d_A) is zero, nonradiative decay rates are zero because the atom is just placed at the mirror. Therefore we get $p = 1$ with $\Gamma_{||} = \Gamma_{||\rm rad} = 0$ and $\Gamma_\perp = \Gamma_{\perp\rm rad} = 2\Gamma_0$. With increasing $d_A(d_0 = 2\ d_A)$, the Zeeman atom interacts with more and more free dipoles in LHM through the dipole-dipole energy transfer, and nonradiative decay rates $\Gamma_{||(\perp)\text{non-rad}}$ increase with d_0 sharply. As $d_0 \approx 0.14\lambda_0$, $\Gamma_{||}$ and $\Gamma_\perp$ reach their maximum values $88\Gamma_0$ and $180\Gamma_0$, consequently p gets its minimum value 0.34 according to Eq. (8). Since the radiative decay rate is much small compared with the total decay rate when $d_0 < 0.5\lambda_0$, the nonradiative decay plays the prominent role in the total decay as the atom-LHM distance is small. Notice that the nonradiative decay originates from the dipole-dipole energy transfer between the atom and the surrounding

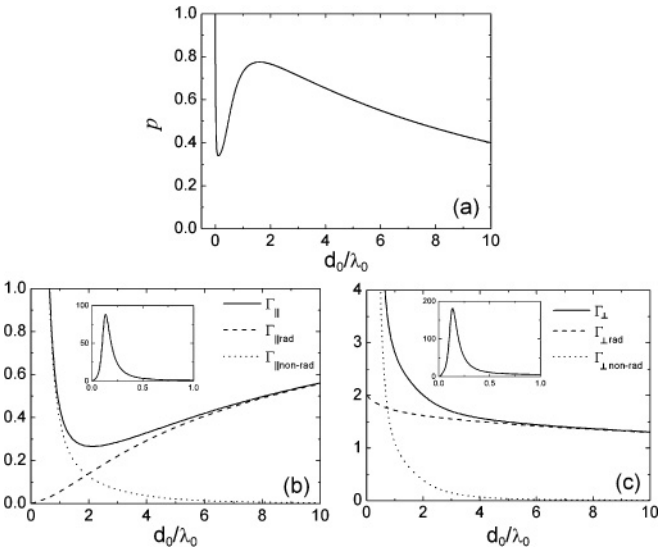

FIG. 4. (a) p as function of d_0, (b) $\Gamma_{||}$ as function of d_0, and (c) $\Gamma_{\perp}$ as function of d_0. The atom is placed in front of a single LHM layer mounted on a single mirror shown in Fig. 3. The insets refer to the enlarged figure of the total decay rate for $d_0 < \lambda$. The reflective coefficients of the mirror are $r_{\mathrm{mir}}^{TE} = -0.99$ and $r_{\mathrm{mir}}^{TM} = 0.99$, and $n_A = -0.999 + i0.003$.

through the Coulomb interaction, and the dipole-dipole energy transfer depends on both the distance and relative orientation between the donor and acceptor [18]. Therefore the maximum $\Gamma_{\perp \mathrm{non-rad}}$ is about twice of the maximum $\Gamma_{||\mathrm{nonrad}}$.

When $d_0 > 0.14\lambda_0 (d_A > 0.07\lambda_0)$, $\Gamma_{||(\perp)\mathrm{nonrad}}$ is approximately proportional to $(d_0/2)^{-3}$, because the Coulomb force between two dipoles is proportional to $(R)^{-3}$ (R is the distance between two dipoles) [18]. With the decreasing of nonradiative decay rate, p reaches its second maximum value 0.8 at $d_0 = 1.2\lambda_0$. The dashed lines and the dotted lines in Fig. 4(b) and (c) illustrate the competition between the radiative decay and the nonradiative decay with the increasing d_0. The nonradiative decay can be omitted completely when $d_0 > 4\lambda_0$, while $\Gamma_{||\mathrm{rad}}(\Gamma_{\perp \mathrm{rad}})$ increases (decreases) with d_0 monotonously. There are two reasons for the deviation of $\Gamma_{||\mathrm{rad}}(\Gamma_{\perp \mathrm{rad}})$ from zero$(2\Gamma_0)$. The major reason is the absorption of the radiative field by dissipation, and the second reason is the deviation of the real part of the refractive index from -1. Consequently, the phase compensation of the LHM is weakened and the Zeeman atom cannot equivalently be placed just at the mirror. So the deviation of $\Gamma_{||\mathrm{rad}}(\Gamma_{\perp \mathrm{rad}})$ from zero $(2\Gamma_0)$ becomes larger with wider d_0, and results in the decrease of p at large d_0.

B. FPC filled with LHM by half (FPCLH)

To improve the quantum interference for larger d_0, we propose to add another wall made of the same LHM and mirror as in the above section on the other side of the atom, as shown in Fig. 5. Here the thickness of the middle layer is twice as long as that of the LHM layers, and the Zeeman atom is placed at the center of the middle layer, i.e., $d_0 = 2\,d_A$, $z_0 = 0$.

The starting point of choosing such a structure is based on the following considerations. In the ideal case $\varepsilon_A = \mu_A = n_A = -1$, the structure is equivalent to a Fabry-Pérot cavity with zero thickness. We know from Fig. 2 that $\Gamma_{||} = 0$ when

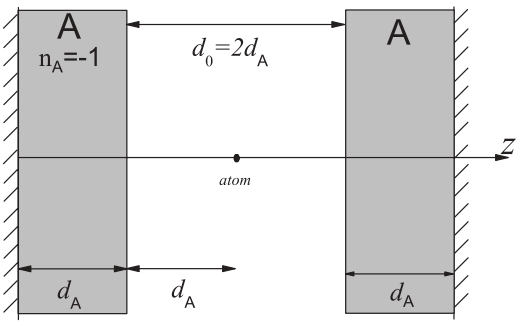

FIG. 5. The scheme of a Fabry-Pérot cavity filled with the LHM layer by half.

the distance between two mirrors is less than half of the wavelength, and then the structure in Fig. 5 can inhibit $\Gamma_{||}$ much more deeply than the structure in Fig. 3 as d_0 increases even if the index of Layer A is deviated from -1. Therefore, p may hold a high value for wider d_0 in the structure of Fig. 5.

We also set the indexes of LHM to be $\varepsilon_A(\omega_0) = \mu_A(\omega_0) = n_A(\omega_0) = -0.999 + i0.003$, and the reflective coefficients of the mirror to be $r_{\mathrm{mir}}^{TE} = -0.99$ and $r_{\mathrm{mir}}^{TM} = 0.99$. The results—$p$, $\Gamma_{||}$, and $\Gamma_{\perp}$ as function of d_0 in such a structure—are shown in Fig. 6.

For the dipole moment parallel to interface, shown in Fig. 6(b), the nonradiative decay rate $\Gamma_{||\mathrm{nonrad}}$ is dominant for $d_0 < \lambda$, and the radiative decay rate is dominant for $d_0 > 4\lambda$. Due to dissipation, the structure of Fig. 5 cannot be rigorously equivalent to be the FPC with zero thickness, and then the radiative decay rate increases with d_0 monotonously. However, as expected, this structure can inhibit $\Gamma_{||}$ much deeper than the single LHM layer mounted on a single mirror (SLSM) when $d_0 > 4\lambda_0$ by comparing Fig. 6(b) with Fig. 4(b).

For the dipole moment normal to interface, both the radiative decay rate and nonradiative decay rate are much

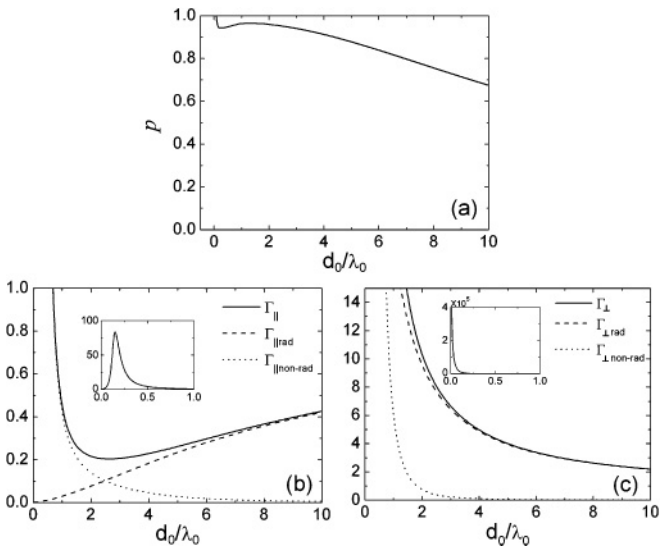

FIG. 6. (a) p as function of d_0, (b) $\Gamma_{||}$ as function of d_0, and (c)$\Gamma_{\perp}$ as function of d_0. The atom is placed in a Fabry-Pérot cavity filled with a LHM layer by half shown in Fig. 5. The reflective coefficients of the mirror are $r_{\mathrm{mir}}^{TE} = -0.99$ and $r_{\mathrm{mir}}^{TM} = 0.99$, and $n_A = -0.999 + i0.003$.

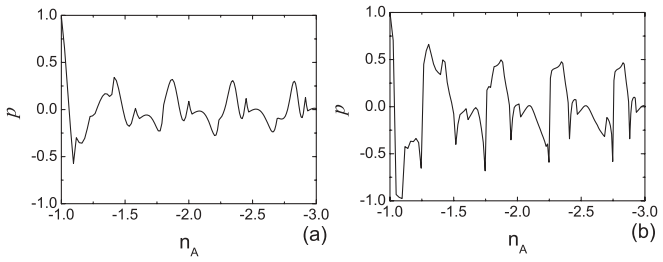

FIG. 7. The relative strength of the quantum interference p as a function of the refractive index n_A. (a) refers to the case of the Zeeman atom in SLSM, and (b) refers to the case in FPCLH. $\mu_A = -1$ is constant. $z_0 = 0$, $d_0 = 2\lambda_0$, and $d_A = \lambda_0$.

higher as $d_0 < \lambda$. Different from the case of SLSM in Fig. 4(c), the saturation of the nonradiative decay rate $\Gamma_{\perp\text{nonrad}}$ only happens when $d_0 \to 0$ and cannot be shown in Fig. 6(c). The reasons are that the Coulomb coupling of the z-direction atomic dipole to the free dipoles in LHM is stronger than that of the x-direction atomic dipole, and LHMs exist on both sides of the atom in FPCLH. On the other hand, the radiative decay rate $\Gamma_{\perp\text{rad}}$ is on the order of $10^2\Gamma_0$ as $d_0 \to 0$ because the z-direction atomic dipole is easy to couple to the leak cavity with zero thickness. Different from the case in SLSM, p is still above 0.9 when $d_0 < \lambda$ in FPCLH even if the dissipation is taken into account. Due to the deeper inhibition of $\Gamma_{||}$ and stronger enhancement of $\Gamma_\perp$ in FPCLH, p can hold a much higher value for wider d_0 in Fig. 6(a) compared with Fig. 4(a). It is clear that p is still 0.7 in FPCLH even if d_0 is $10\lambda_0$.

Though the dissipation of LHM has a destructive influence on the quantum interference of the Zeeman atom in the above two structures, the quantum interference p is still larger than that in the FPC [7], multilayer dielectric medium [8], and one-dimensional photonic crystals [9] when the distance between the atom and surrounding is larger than half of the wavelength.

Finally, we discuss the influence of the refractive index of LHM on the quantum interference. We set the permeability $\mu_A = -1$, and change the permittivity ε_A from -1 to -9. The relative strength of the quantum interference p of the atom in SLSM and FPCLH as a function of refractive index n_A is shown in Fig. 7.

From Fig. 7, p damps accompanying oscillations with the deviation of n_A from -1. p reaches the maximum 1 only when $n_A = -1$, in which the phase compensation of LHM works. If n_A deviates from -1, the effect of phase compensation is still work, but the atom is no longer equivalent to be placed just at the mirror, so the amplitude of p for $n_A \neq -1$ is smaller than that for $n_A = -1$ but is larger than that of atom in F-P cavity. In addition, the amplitude of p for atom in FPCLH is stronger than that in SLSM.

IV. THE INTERFERENCE BETWEEN TWO SPATIAL ORTHOGONAL DIPOLES

In Secs. II and III, we discussed the quantum interference between two phase orthogonal dipoles, i.e., left-rotating polarized dipole and right-rotating polarized dipole. In mathematics, the left rotating-polarized dipole and right-polarized dipole can be equivalent to two spatial perpendicular linear polarized dipoles. For example, the transformation of $\boldsymbol{\varepsilon}_+ = (\boldsymbol{e}_z + i\boldsymbol{e}_x)/\sqrt{2} \to \boldsymbol{e}_1 = (\boldsymbol{e}_z + \boldsymbol{e}_x)/\sqrt{2}$ and $\boldsymbol{\varepsilon}_- = (\boldsymbol{e}_z - i\boldsymbol{e}_x)/\sqrt{2} \to \boldsymbol{e}_2 = (\boldsymbol{e}_z - \boldsymbol{e}_x)/\sqrt{2}$ has no influence on the results of Sec. III. In this section, we focus on the case in which two dipoles are spatially perpendicular to each other, and aim to find the optimum orientation of these two dipoles to get the maximum quantum interference in a certain environment. This question is also relevant to finding the optimum orientation of the normal line of the one-dimensional structure relative to the rotation polarized ε_+ and ε_-. The dipole moment operator considered here can be expressed as

$$\boldsymbol{d} = d(A_{13}\boldsymbol{e}_1 + A_{23}\boldsymbol{e}_2) + \text{H.c.}, \tag{14}$$

$$\boldsymbol{e}_1 = (\sin\theta_1\cos\phi_1\boldsymbol{e}_x + \sin\theta_1\sin\phi_1\boldsymbol{e}_y + \cos\theta_1\boldsymbol{e}_z), \tag{15}$$

$$\boldsymbol{e}_2 = (\sin\theta_2\cos\phi_2\boldsymbol{e}_x + \sin\theta_2\sin\phi_2\boldsymbol{e}_y + \cos\theta_2\boldsymbol{e}_z). \tag{16}$$

We set the orientation angle $\phi_1 = 0$ to simplify the analysis, which means $\boldsymbol{e}_1$ varies only on the x-z plane. The geometrical orientation of dipoles $\boldsymbol{e}_1$ and $\boldsymbol{e}_2$ is shown in Fig. 8.

Owing to $\boldsymbol{e}_1 \perp \boldsymbol{e}_2$, we get the relationship between θ_1, θ_2, and ϕ_2 as

$$\tan\theta_2\cos\phi_2 = -\frac{1}{\tan\theta_1}. \tag{17}$$

Under the approximation $\omega_1 \approx \omega_2 = \omega_0$, the spontaneous decay rates $\gamma_{1,2}$ and the quantum interference $\kappa_{1,2}$ in the anisotropic environment of $G_{xx} = G_{yy} \neq G_{zz}$ should be rewritten as

$$\gamma_1 = d^2\omega_0^2\boldsymbol{e}_1\text{Im}\boldsymbol{G}(\boldsymbol{r}_0, \boldsymbol{r}_0, \omega_0)\boldsymbol{e}_1 = \cos^2\theta_1\Gamma_\perp + \sin^2\theta_1\Gamma_{||}, \tag{18}$$

$$\gamma_2 = d^2\omega_0^2\boldsymbol{e}_2\text{Im}\boldsymbol{G}(\boldsymbol{r}_0, \boldsymbol{r}_0, \omega_0)\boldsymbol{e}_2 = \cos^2\theta_2\Gamma_\perp + \sin^2\theta_2\Gamma_{||}, \tag{19}$$

$$\begin{aligned}\kappa &= \kappa_{1,2} = d^2\omega_0^2\boldsymbol{e}_1\text{Im}\boldsymbol{G}(\boldsymbol{r}_0, \boldsymbol{r}_0, \omega_0)\boldsymbol{e}_2 \\ &= \sin\theta_1\sin\theta_2\cos\phi_2\Gamma_{||} + \cos\theta_1\cos\theta_2\Gamma_\perp.\end{aligned} \tag{20}$$

The relative intensity of the quantum interference in such case is

$$\begin{aligned}p = \kappa/\sqrt{\gamma_1\gamma_2} &= \frac{\sin\theta_1\sin\theta_2\cos\phi_2\Gamma_{||} + \cos\theta_1\cos\theta_2\Gamma_\perp}{\sqrt{(\sin^2\theta_1\Gamma_{||} + \cos^2\theta_1\Gamma_\perp)(\sin^2\theta_2\Gamma_{||} + \cos^2\theta_2\Gamma_\perp)}} \\ &= \frac{\cos\theta_1\cos\theta_2(1 - \Gamma_{||}/\Gamma_\perp)}{\sqrt{[\cos^2\theta_1(1 - \Gamma_{||}/\Gamma_\perp) + \Gamma_{||}][\cos^2\theta_2(1 - \Gamma_{||}/\Gamma_\perp) + \Gamma_{||}/\Gamma_\perp]}}.\end{aligned} \tag{21}$$

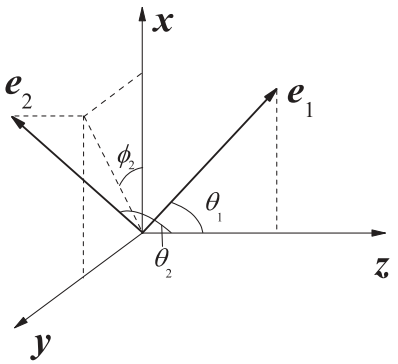

FIG. 8. The geometrical orientation of dipoles $\boldsymbol{e}_1$ and $\boldsymbol{e}_2$.

From Eq. (21), the value of p depends on both the orientation angles of two dipoles and the ratio of $\Gamma_{||}$ to $\Gamma_{\perp}$.

According to the discussion in Sec. II, the strongest quantum interference requires the equality between $\gamma_{1,2}$ and $\kappa_{1,2}$. The sole condition fitting such a requirement is that either $\Gamma_{\perp}$ or $\Gamma_{||}$ is zero. However, the results of Sec. III tell us that it is impossible to get either $\Gamma_{\perp}$ or $\Gamma_{||}$ to be zero if the LHM contains dissipation. Therefore the key emphasis in this section is to find the optimum orientation of such two spatial orthogonal dipoles to get the maximum quantum interference in a certain environment.

Below, we will calculate the variation of p as a function of orientation angles ϕ_2 and θ_1 [while the orientation angle θ_2 is determined by Eq. (17)] in different environments marked by certain $\Gamma_{||}/\Gamma_{\perp}$.

We first consider the case of $\Gamma_{||} = 0.706\Gamma_0$ and $\Gamma_{\perp} = 4\Gamma_0$. Here the values of the decay rates are not the emphasis, the key point is their ratio $\Gamma_{||}/\Gamma_{\perp}$. Keeping the same ratio and multiplying a common number to both $\Gamma_{||}$ and $\Gamma_{\perp}$ does not change the result according to Eq. (21). From Fig. 9, there are two common values of ϕ_2 to make $|p| = 0$ for all θ_1, which are $\phi_2 = 90^\circ$ and $\phi_2 = 270^\circ$. The cases of $\phi_2 = 90^\circ$ and $\phi_2 = 270^\circ$ mean that $\boldsymbol{e}_2 = \pm\boldsymbol{e}_z$.

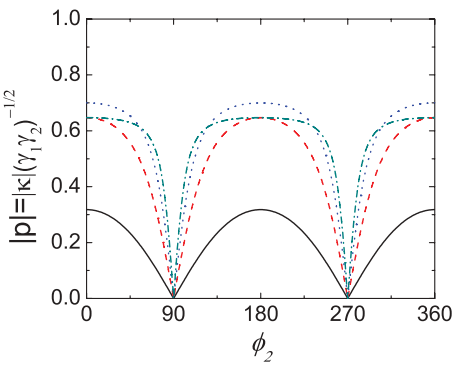

FIG. 9. (Color online) the absolute value of the degree of quantum interference $|p|$ as a function of orientation angle ϕ_2 for $\theta_1 = 10^\circ$ (black line), $\theta_1 = 30^\circ$ (dashed/red line), $\theta_1 = 45^\circ$ (dotted/blue line), and $\theta_1 = 60^\circ$ (dash-dotted/dark cyan line). Here $\Gamma_{||} = 0.706\Gamma_0$ and $\Gamma_{\perp} = 4\Gamma_0$. The case of $\theta_1 = 180^\circ - a$ is the same as the case of $\theta_1 = a$. $a \in [0, 90^\circ]$.

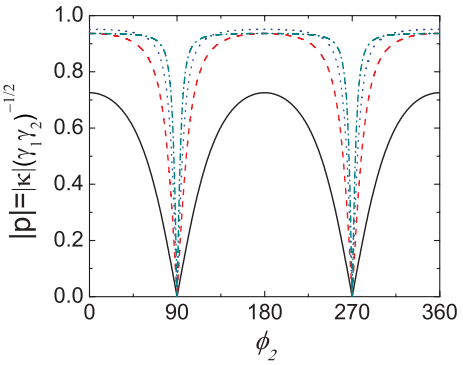

FIG. 10. (Color online) the absolute value of the degree of quantum interference $|p|$ as a function of orientation angle ϕ_2 for $\theta_1 = 10^\circ$ (black line), $\theta_1 = 30^\circ$ (dashed/red line), $\theta_1 = 45^\circ$ (dotted/blue line), and $\theta_1 = 60^\circ$ (dash-dotted/dark cyan line). Here $\Gamma_{||} = 0.1\Gamma_0$ and $\Gamma_{\perp} = 4\Gamma_0$. The case of $\theta_1 = 180^\circ - a$ is the same as the case of $\theta_1 = a$. $a \in [0, 90^\circ]$.

However, there are two common values of ϕ_2 for all θ_1 to reach the relative maximum $|p|$, which are $\phi_2 = 0^\circ$ and $\phi_2 = 180^\circ$. Among all the groups of ϕ_2 and θ_1, groups ($\phi_2 = 0^\circ$, $\theta_1 = 45^\circ$) and ($\phi_2 = 180^\circ$, $\theta_1 = 45^\circ$) lead to the absolute maximum value of $|p| = 0.700$, and will generate the maximum quantum interference for the environment of $\Gamma_{||} = 0.706\Gamma_0$ and $\Gamma_{\perp} = 4\Gamma_0$.

Then we check the case of $\Gamma_{||} = 0.1\Gamma_0$ and $\Gamma_{\perp} = 4\Gamma_0$ in Fig. 10. Similarly to Fig. 9, the groups ($\phi_2 = 0^\circ$, $\theta_1 = 45^\circ$) and ($\phi_2 = 180^\circ$, $\theta_1 = 45^\circ$) lead to the absolute maximum value of $|p| = 0.951$. And when $\phi_2 = 90^\circ$ and $\phi_2 = 270^\circ$, the quantum interference disappears even if the difference between $\Gamma_{||}$ and $\Gamma_{\perp}$ is large here. Comparing Fig. 10 with Fig. 9, the maximum $|p|$ in Fig. 10 is much higher than that in Fig. 9. The absolute maximum $|p|$ in Figs. 9 and 10 satisfy the formula $|p|_{max} = |(\Gamma_{\perp} - \Gamma_{||})/(\Gamma_{\perp} - \Gamma_{||})|$, which are just the $|p|$ of the Zeeman three-level atom with $\boldsymbol{\varepsilon}_{\pm} = (\boldsymbol{e}_z \pm i\boldsymbol{e}_x)/\sqrt{2}$ in these environments.

In the Appendix, we analytically prove the above conclusion that, for an anisotropic environment with $G_{xx} = G_{yy} \neq G_{zz}$, the quantum interference between two spatial orthogonal dipoles disappears when $\phi_2 = 90^\circ$ or 270° and the quantum interference reaches the absolute maximum when $\theta_1 = 45^\circ$ or 135° and $\phi_2 = 0$ or 180°. It should be noticed that $\phi_2 = 90^\circ$ or 270° means that $\boldsymbol{e}_2$ is along the y-axis, and $\boldsymbol{e}_1$ is on the x-z plane. Because the x-y plane is isotropic, $\boldsymbol{e}_2$ has no interaction with the x-component of $\boldsymbol{e}_1$, in addition $\boldsymbol{e}_2$ cannot couple to the z-component of $\boldsymbol{e}_1$, and then no quantum interference happens for such cases. However $\theta_1 = 45^\circ$ or 135° and $\phi_2 = 0^\circ$ or 180° mean that $\boldsymbol{e}_1$ and $\boldsymbol{e}_2$ are both in the x-z plane and their z-component has the same amplitude with the x-component. The absolute maximum $|p|$ when $\theta_1 = 45^\circ$ or 135° and $\phi_2 = 0^\circ$ or 180° equals to $|p|$ of the Zeeman three-level atom with $\varepsilon_{\pm} = (\boldsymbol{e}_z \pm i\boldsymbol{e}_x)/\sqrt{2}$ in the same environment. As the SLSM and FPCLH can provide much higher $|p|$ for the Zeeman atom for much wider space than the ordinary materials, the quantum interference between two spatial orthogonal dipoles can also be enhanced in SLSM and FPCLH when their dipole orientations are adjusted into

the optimum orientations $\theta_1 = 45^\circ$ or 135° and $\phi_2 = 0^\circ$ or 180°.

V. CONCLUSION

As a conclusion of this paper, LHM have been used to enhance the quantum interference between two orthogonal dipoles due to the phase compensation. For a lossless ideal LHM, the Zeeman atom in a single LHM layer mounted on a single mirror (SLSM) is equivalent to being placed at the mirror, and the Zeeman atom in the FPC filled with the LHM layer by half (FPCLH) is equivalent to be placed in a zero-thickness FPC, and then complete quantum interference can be achieved for arbitrary distance between the atom and the ideal LHM. The influence of the dissipation of LHM has been considered, and the competition between radiative decay and nonradiative decay has also been studied in detail. We find the dissipation of LHM can weaken the quantum interference for larger d_0, but the strong quantum interference can be generated in FPCLH even if the distance between the atom and LHM is larger than five wavelengths. Additionally, with the equivalence of the rotation polarized $\boldsymbol{\varepsilon}_+$ and $\boldsymbol{\varepsilon}_-$ to two spatial orthogonal dipoles, we address the optimum orientation of two orthogonal dipoles which can be used to realize the maximum interference in an anisotropic environment of $G_{xx} = G_{yy} \neq G_{zz}$. This object is also equivalent to find the optimum orientation of a normal line of one-dimensional structure relative to rotationally polarized $\boldsymbol{\varepsilon}_+$ and $\boldsymbol{\varepsilon}_-$. The enhancement of quantum interference for a large distance may have a potential application in the designing of microsize devices.

ACKNOWLEDGMENTS

This work was supported in part by the Foundation of the Ministry of Science and Technology (Nos. 2006CB921701 and 2007CB13201), the National Science Foundation of China (Nos. 10674103 and 10904113), and the NCET-06-0384. Program for Young Excellent Talents in Tongji University (No. 2009KJ068).

APPENDIX: THE OPTIMUM ORIENTATION OF TWO ORTHOGONAL DIPOLES TO REACH THE MAXIMUM OF $|p|$

Part (i): If θ_1 is fixed, what is the value of ϕ_2 to reach the relative maximum and minimum of $|p|$?

The expression of p for two spatial orthogonal dipoles is shown in Eq. (A1) as

$$p = \frac{\cos\theta_1 \cos\theta_2(\Gamma_\perp - \Gamma_{||})}{\sqrt{[\cos^2\theta_1(\Gamma_\perp - \Gamma_{||}) + \Gamma_{||}][\cos^2\theta_2(\Gamma_\perp - \Gamma_{||}) + \Gamma_{||}]}}. \tag{A1}$$

To derivate the above formation, the orthogonal condition, Eq. (17) in which $\cos\phi_2 = -1/(\tan\theta_1 \tan\theta_2)$, has been used. Let $a = \Gamma_{||}/(\Gamma_\perp - \Gamma_{||})$ ($a \geqslant 0$ due to $\Gamma_\perp > \Gamma_{||} \geqslant 0$), we get the square of p as

$$p^2 = \frac{1}{\left(1 + \frac{a}{\cos^2\theta_1}\right)\left(1 + \frac{a}{\cos^2\theta_2}\right)}. \tag{A2}$$

With Eq. (17), we get

$$\cos^2\theta_2 = \frac{1}{1 + \tan^2\theta_2} = \frac{1}{1 + \frac{1}{\tan^2\theta_1 \cos^2\phi_2}}, \tag{A3}$$

then p^2 can be rewritten as

$$p^2 = \frac{1}{\left(1 + \frac{a}{\cos^2\theta_1}\right)\left(1 + a + \frac{a}{\tan^2\theta_1 \cos^2\phi_2}\right)}. \tag{A4}$$

It is clear that, if θ_1 is fixed, p^2 reaches the relative maximum value when $\phi_2 = 0, \pi$. However, p^2 reaches the minimum value 0 when $\phi_2 = \frac{\pi}{2}, \frac{3\pi}{2}$.

Part (ii): What is the group of (θ_1,ϕ_2) that can reach the absolute maximum of $|p|$?

The previous part shows that, for certain θ_1, p^2 reaches the relative maximum value when $\phi_2 = 0, \pi$. Now we want to ascertain the group (θ_1,ϕ_2) to make p^2 the absolute maximum. Following the above part, the value of ϕ_2 should be $\phi_2 = 0, \pi$, and the corresponding p^2 is

$$p^2 = \frac{1}{\left(1 + \frac{a}{\cos^2\theta_1}\right)\left(1 + \frac{a}{\sin^2\theta_1}\right)}. \tag{A5}$$

Let $x = \cos^2\theta_1$ ($x \in [01]$), the denominator of Eq. (A5) can be simplified and be defined as y by

$$\begin{aligned} y &= \left(1 + \frac{a}{x}\right)\left(1 + \frac{a}{1-x}\right) \\ &= 1 + \frac{a}{x} + \frac{a}{1-x} + \frac{a^2}{x(1-x)}. \end{aligned} \tag{A6}$$

The derivative of y, with respect to x, is

$$y' = a\left[\frac{1}{(1-x)^2} - \frac{1}{x^2} - \frac{a(1-2x)}{x^2(1-x)^2}\right]. \tag{A7}$$

It is well known that $y(x_0)$ is an absolute extremum of y when $y'(x_0) = 0$. Such $y(x_0)$ will be the absolute maximum if $y''(x_0) < 0$, or be the absolute minimum if $y''(x_0) > 0$. By solving the equation of $y'(x_0) = 0$, we get $x_0 = 1/2$.

The second derivative of y, with respect to x, is

$$\begin{aligned} y'' = a\Bigg\{&\frac{2}{(1-x)^3} + \frac{2}{x^3} \\ &+ a\frac{2x(1-x) + (1-2x)[2(1-x) - 2x]}{x^3(1-x)^3}\Bigg\}. \end{aligned} \tag{A8}$$

Inserting $x_0 = 1/2$ into Eq. (A8), we get

$$y''(x_0) = a(2^4 + 2^4 + 2^5 a) = 2^5 a(1 + a) > 0. \tag{A9}$$

As $y'(x_0) = 0$ and $y''(x_0) > 0$, y takes the absolute minimum at $x_0 = 1/2$. Consequently, ascos$^2\theta_1 = 1/2$, p^2 takes the maximum value.

So we have proved that the absolute value of p for two spatial orthogonal dipoles gets the maximum value when $\theta_1 = \pi/4$ or $3\pi/4$ and $\phi_2 = 0$ or π.

[1] G. Alzetta, A. Gozzini, L. Moi, and G. Orriols, Nuovo Cimento B **36**, 5 (1976); H. R. Gray, R. M. Whitley, and C. R. Stroud, Phys. Rev. A **14**, 1498 (1976); P. M. Radmore and P. L. Knight, J. Phys. B **15**, 561 (1982).

[2] A. Javan, Phys. Rev. **107**, 1579 (1956); V. Arkhipkin and Yu Heller, Phys. Lett. **A98**, 12 (1983); M. O. Scully, S. Y. Zhu, and A. Gavrielides, Phys. Rev. Lett. **62**, 2813 (1989); M. O. Scully, S. Y. Zhu, and H. Fearn, Z. Phys. D **22**, 471 (1992).

[3] S. E. Harris, J. E. Field, and A. Imamoglu, Phys. Rev. Lett. **64**, 1107 (1990); K. H. Hahn, D. A. King, and S. E. Harris, *ibid.* **65**, 2777 (1990); K. Hakuta, L. Marmet, and B. P. Stoicheff, *ibid.* **66**, 596 (1991).

[4] S. Menon and G. S. Agarwal, Phys. Rev. A **61**, 013807 (1999); F. L. Li and S. Y. Zhu, Opt. Commun. **162**, 155 (1999).

[5] P. Zhou and S. Swain, Phys. Rev. Lett. **77**, 3995 (1996); C. H. Keitel, *ibid.* **83**, 1307 (1999); F. L. Li and S. Y. Zhu, Phys. Rev. A **59**, 2330 (1999).

[6] E. Paspalakis, N. J. Kylstra, and P. L. Knight, Opt. Commun. **152**, 293 (1998).

[7] G. S. Agarwal, Phys. Rev. Lett. **84**, 5500 (2000).

[8] G. X. Li, F. L. Li, and S. Y. Zhu, Phys. Rev. A **64**, 013819 (2001).

[9] J. P. Xu, L. G. Wang, Y. P. Yang, Q. Lin, and S. Y. Zhu, Opt. Lett. **33**, 2005 (2008).

[10] Y. P. Yang, J. P. Xu, H. Chen, and S. Y. Zhu, Phys. Rev. Lett. **100**, 043601 (2008).

[11] V. G. Veselago, Sov. Phys. Usp. **10**, 509 (1968).

[12] J. B. Pendry, Phys. Rev. Lett. **85**, 3966 (2000).

[13] N. Engheta, IEEE Antennas Wireless Propag. Lett. **1**, 10 (2002); L. F. Shen, S. L. He, and S. S. Xiao, Phys. Rev. B **69**, 115111 (2004); H. Q. Li, J. M. Hao, L. Zhou, Z. Y. Wei, L. K. Gong, H. Chen, and C. T. Chan, App. Phys. Lett. **89**, 104101 (2006).

[14] J. Kästel and M. Fleischhauer, Phys. Rev. A **71**, 011804(R) (2005).

[15] D. R. Smith, W. J. Padilla, D. C. Vier, S. C. Nemat-Nasser, and S. Schultz, Phys. Rev. Lett. **84**, 4184 (2000); S. Zhang, W. Fan, B. K. Minhas, A. Frauenglass, K. J. Malloy, and S. R. J. Brueck, *ibid.* **94**, 037402 (2005); S. Zhang, W. Fan, N. C. Panoiu, K. J. Malloy, R. M. Osgood, and S. R. J. Brueck, *ibid.* **95**, 137404 (2005); M. S. Wheeler, J. S. Aitchison, and M. Mojahedi, Phys. Rev. B **73**, 045105 (2006).

[16] S. Zhang, W. J. Fan, N. C. Panoiu, K. J. Malloy, R. M. Osgood, and S. R. J. Brueck, Phys. Rev. Lett. **95**, 137404 (2005); S. Zhang, W. J. Fan, B. K. Minhas, A. Frauenglass, K. J. Malloy, and S. R. J. Brueck, *ibid.* **94**, 037402 (2005); H. J. Lezec, J. A. Dionne, and H. A. Atwater, Science **316**, 430 (2007); G. Dolling, M. Wegener, C. M. Soukoulis, and S. Linden, Opt. Lett. **32**, 53 (2007); G. Dolling, M. Wegener, and S. Linden, *ibid.* **32**, 551 (2007).

[17] M. S. Tomas, Phys. Rev. A **51**, 2545 (1995).

[18] H. T. Dung, L. Knöll, and D. G. Welsch, Phys. Rev. A **62**, 053804 (2000); S. Scheel, L. Knöll, and D. G. Welsch, *ibid.* **60**, 4094 (1999); M. S. Tomas and Z. Lenac, *ibid.* **56**, 4197 (1997).